

UNIVERSIDADE FEDERAL DO PAMPA

MATHEUS CASTRO NICOLAU DA SILVA

**THE INFLUENCE OF
KELVIN-HELMHOLTZ INSTABILITY
IN A MIXING LAYER: A SIMPLE
MODEL FOR THE STUDY OF FIRE
SAFETY BETWEEN TWO PARALLEL
WALLS**

**Alegrete
December 2020**

MATHEUS CASTRO NICOLAU DA SILVA

**THE INFLUENCE OF
KELVIN-HELMHOLTZ INSTABILITY
IN A MIXING LAYER: A SIMPLE
MODEL FOR THE STUDY OF FIRE
SAFETY BETWEEN TWO PARALLEL
WALLS**

Trabalho de Conclusão de Curso apresentado ao curso de Bacharelado em Engenharia Civil como requisito parcial para a obtenção do grau de Bacharel em Engenharia Civil.

Advisor: Cesar Flaubiano da Cruz Cristaldo

**Alegrete
December 2020**

Ficha catalográfica elaborada automaticamente com os dados fornecidos
pelo(a) autor(a) através do Módulo de Biblioteca do
Sistema GURI (Gestão Unificada de Recursos Institucionais) .

S586t Silva, Matheus Castro Nicolau da
The influence of Kelvin-Helmholtz instability in a mixing
layer: a simple model for study of fire safety between two
parallel walls / Matheus Castro Nicolau da Silva.
40 p.

Trabalho de Conclusão de Curso(Graduação)-- Universidade
Federal do Pampa, ENGENHARIA CIVIL, 2020.

"Orientação: Cesar Flaubiano da Cruz Cristaldo".

1. Kelvin-Helmholtz. 2. Vortices. 3. Temperature gradients.
4. Stability. 5. Instability. I. Título.

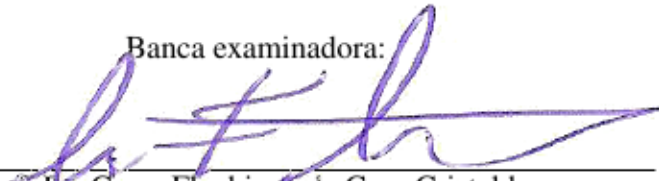
MATHEUS CASTRO NICOLAU DA SILVA

**THE INFLUENCE OF KELVIN-
HELMHOLTZ INSTABILITY IN A
MIXING LAYER: A SIMPLE MODEL
FOR THE STUDY OF FIRE SAFETY
BETWEEN TWO PARALLEL WALLS**

Trabalho de Conclusão de Curso apresentado ao curso de Bacharelado em Engenharia Civil como requisito parcial para a obtenção do grau de Bacharel em Engenharia Civil.

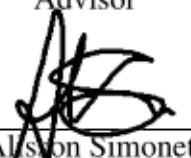
Trabalho de Conclusão de Curso defendido e aprovado em: 4 de dezembro de 2020.

Banca examinadora:



Prof. Dr. Cesar Flaubiano da Cruz Cristaldo

Advisor



Prof. Dr. Alisson Simonetti Milani
Universidade Federal do Pampa



Prof. Dr. Rafael Maronezo
Universidade Federal do Pampa

ACKNOWLEDGEMENTS

I would like to express my sincere thanks to Dr. Cesar Cristaldo, for the motivation, support, for calming down, for not letting me give up. His teachings changed the course of my life and this will always be remembered.

Many thanks to my friends, for helping me and making my days better.

Especial thanks to Ana Paula Machado, for being by my side during the entire graduation.

And nothing would be possible without my parents' unconditional support, who I love.

"O, let not the flame die out!
Cherished age after age in its dark caverns,
In its holy temples cherished.
Fed by pure ministers of love
Let not the flame die out.
Within thy body I behold it flicker,
Through the slight husk I feel quick fire leap-
ing
O, let not the flame die out."
— Edward Carpenter

ABSTRACT

A hydrodynamic stability study was carried out to investigate Kelvin-Helmholtz vortices development. In order to be able to capture the small variations caused in the flow and the response that it will give to these disturbances, whether or not it may evolve to an unstable regime, it is necessary to use high-order, low dissipation and low dispersion numerical methods. As a parametric model, the governing equations were deduced in their dimensionless form so that it could be carried out based on the principle of dynamic similarity. In order to study reactive flow in the future, second order terms such as viscous and heat conduction had to be implemented. The influence of strong temperature gradients on the formation of vortices and their respective amplification rate of the disturbances was verified. For future work with the mixing layer, the governing equations for reactive flows with diffusive flames were deduced through the Shvab-Zel'Dovich formulation.

Keywords: Kelvin-Helmholtz. Vortices. Temperature gradients. Stability. Instability.

RESUMO

Foi realizado um estudo de estabilidade hidrodinâmica para investigar o desenvolvimento de vórtices de Kelvin-Helmholtz. Para que seja possível capturar as pequenas variações provocadas no escoamento e a resposta que este dará a estas perturbações, podendo ou não evoluir para regime instável, é necessário recorrer a métodos numéricos de alta ordem, baixa dissipação e baixa dispersão. Por ser um modelo paramétrico, as equações governantes foram deduzidas em sua forma adimensional para que se pudesse fazer análises baseadas no princípio da similaridade dinâmica. Objetivando futuramente o estudo de um escoamento reativo, os termos de segunda ordem como os viscosos e de condução de calor, tiveram que ser implementados. Foi verificada a influência de fortes gradientes de temperatura na formação de vórtices e sua respectiva taxa de amplificação das perturbações. Para futuros trabalhos com camada de mistura, foram deduzidas as equações governantes para escoamentos reativos com chamas difusivas através da formulação de Shvab-Zel'Dovich.

Palavras-chave: Kelvin-Helmholtz, Vórtices, Gradientes de temperatura, Estabilidade, Instabilidade.

LIST OF FIGURES

Figure 1 Simplified representation of a fire plume (circular geometry).	12
Figure 2 Fire plume.....	13
Figure 3 Sketch of: zoom in the flame region, indicating the differences in velocity and density (left); sketch of vortex roll-up with unstable and stable regions (right). Density $\rho_1 < \rho_2$	13
Figure 4 Kelvin-Helmholtz instability in shear flow.....	14
Figure 5 Problem schematic: mixing layer	15
Figure 6 Representation of a fluid element and the forces acting on it's surfaces	17
Figure 7 Mesh representation showing interest domain and buffer zone.....	21
Figure 8 Growth rate versus frequency ω , comparison between linear stability analysis and Euler numerical simulation.	22
Figure 9 Reference flow vorticity distribution	24
Figure 10 Reference flow pressure distribution	25
Figure 11 Reference flow normal velocity component distribution.....	25
Figure 12 Vorticity Distribution for Re=10000. In figure (a) has values for $T_1 = 1$, $T_2 = 0.5$ and $\omega = 0.8$. Figure (b) has values for $T_1 = 1$, $T_2 = 1$ and $\omega = 1$. Figure (c) has values for $T_1 = 1$, $T_2 = 2$ and $\omega = 1.2$	26
Figure 13 Pressure distribution for Re=10000. The figure (a) has values for $T_1 = 1$ and $T_2 = 0.5$, $\omega = 0.8$. Figure (b) has values for $T_1 = 1$ and $T_2 = 1$, $\omega = 1$ and figure (c) $T_1 = 1$ and $T_2 = 2$, $\omega = 1.2$	27
Figure 14 Normal velocity component for Re=10000. Figure (a) has values for $T_1 = 1$ and $T_2 = 0.5$, $\omega = 0.8$. Figure (b) has values for $T_1 = 1$ and $T_2 = 1$, $\omega = 1$ and figure (c) has values for $T_1 = 1$ and $T_2 = 2$, $\omega = 1.2$	28
Figure 15 Linear Stability Theory results. Effect of Temperature gradient. $T_1 = 1$ through $T_2 = 0.1$ to 10 using Re=10000.	29

CONTENTS

1 INTRODUCTION	10
1.1 General Objectives	11
1.2 Specific Objectives	11
2 LITERATURE REVIEW	12
2.1 Fire modelling	12
2.2 Reacting Mixing Layer	14
3 METHODOLOGY	15
3.1 Governing Equations	16
3.1.1 Viscosity and thermal conductivity terms	17
3.2 Adimensionalization	18
3.2.1 Continuity	19
3.2.2 Momentum.....	20
3.2.3 Energy	20
3.3 Numerical methodology	20
3.4 Code Verification	21
4 RESULTS AND DISCUSSION	23
4.1 Parameters	23
4.2 Reference flow results	24
4.3 Strong Temperature Gradient Cases	26
4.4 Linear Stability Theory Analysis	28
5 CONCLUSIONS	30
REFERENCES	31
APPENDIX A — SHVAB-ZEL'DOVICH FORMULATION FOR DIFFU- SION FLAMES	34
A.1 Conservation of species equation	34
A.2 Energy equation with reactive terms	35
A.3 Adimensionalization	36
A.3.1 Energy equation with chemical reaction	37
A.3.2 Chemical Species	38
A.4 Eliminating the chemical reaction from the energy equation	38

1 INTRODUCTION

The successful design of fire safety engineers are required to analyze structures to ensure acceptable levels of safety. Modellers explicitly consider a small part of a total system (e.g. a single room in a building or a short section of a tunnel) and expand conclusions to the entire system.

Some engineering problems requires fast analysis and requires the use of parametric investigation for different hypothesis of the flow, as the compressible mixing layer, a model problem for the analysis of high speed air breathing propulsion problems such as reactant mixing in a combustion chamber, noise generation and mixture of sanility, pollution and other properties in fluids. In both cases to parallel streams at different velocities may be composed of different chemical species or with large temperature differences and properties variation may result in significant differences in flow stability characteristics such as growth rates. This work investigates how viscous terms and temperature gradients affects the development of Kelvin-Helmholtz instability.

The research on the stability of binary mixing layers at the Instituto de Aeronáutica e Espaço (IAE) started in 2006 with the Masters' thesis of Salemi (2006) (SALEMI; MENDONCA, 2008) and Quirino (2006). Were investigated hydrodynamic stability theory to study binary mixing layers in compressible flow and direct numerical simulation methods to solve the compressible Navier-Stokes equations, to study the effect of strong heat sources on the stability of the mixing layer.

Other works where conducted on more complex models of double mixing layers or mixing layers modified by jets and wakes (MENDONÇA, 2010; SOUZA, 2011; SOUZA; ALVES; MENDONCA, 2014; MENDONCA, 2014; SOARES; FILHO; MENDONcA, 2014; FERNANDES; FREITAS; MENDONcA, 2014; FREITAS; FERNANDES; MENDONCA, 2014; MANCO, 2014; MANCO; MENDONCA, 2014).

The present investigation extend these previous work using some of the methodologies developed by the group for the study of more complex mixing layer configurations. Thus, the diffusion is added on the governing equations with objective of include the combustion in the future.

1.1 General Objectives

The objective of this work is to understand the characteristics of compressible, binary, parallel reactant streams, typically found in fire plume. The aim is to understand the mechanisms of generation, propagation and interaction of disturbances in the velocity, entropy and acoustic fields which are associated to instability problems in combustion devices and may hinder their performance. The long term goal is to understand the influence of instability problems to prevent set of practices intended to reduce the destruction caused by fire (fire safety). The influence of important parameters in the development of thermal, hydrodynamic and acoustic disturbances in terms of frequencies, wave-numbers and amplification rates will be investigated. These parameters are the Mach number, the temperature and velocity ratios between two parallel walls.

1.2 Specific Objectives

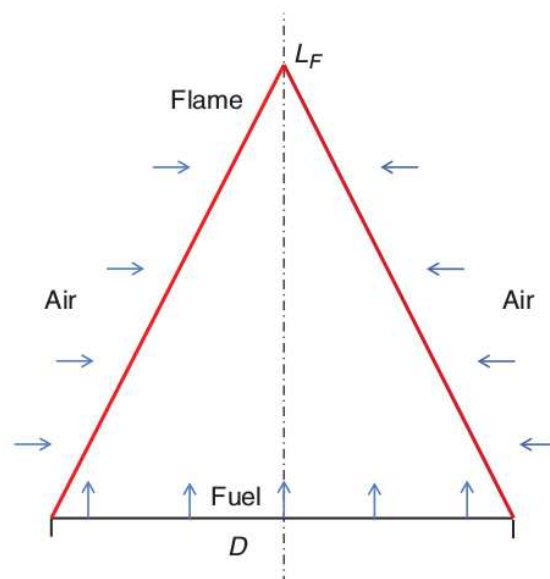
The main objective of this work is to study the influence of Kelvin-Helmholtz instability between two parallel reactant streams at different velocity and temperature (or density). This configuration is similar to a fire plume when there are local differences in velocity in the flow. The fluid flow is composed by fuel and oxidant and a flame is established between the reactant streams. Thus the influence of the formed vortices on the transfer of heat between the two parallel walls is analyzed.

2 LITERATURE REVIEW

2.1 Fire modelling

Generally, fire plumes are modeled by a simplified model, see Fig.1. The flame shape is represented by cone, in which, L_F is the length and D is the flame diameter. These approximations are satisfactory, only, for the first global discussion.

Figure 1 – Simplified representation of a fire plume (circular geometry).

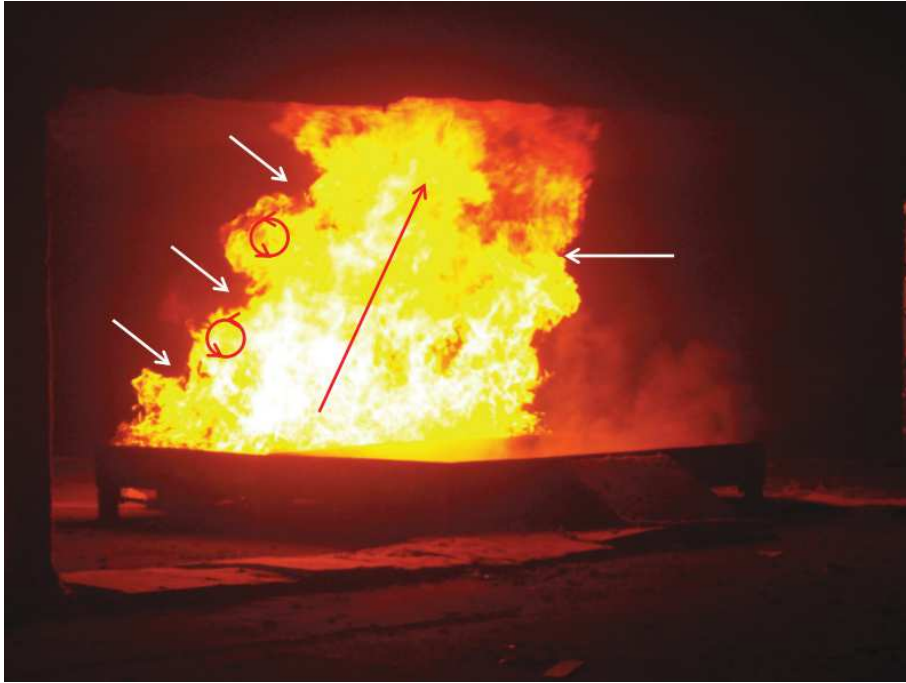


Fonte: (MERCİ; BEJİ, 2016)

In real fire plumes the turbulence is involved. Turbulence is generated by instabilities. These instabilities are generated by density differences and the resulting flow. Figure (2) provides an illustration of a real fire plume, with rectangular fuel pool. The white arrows indicate ‘unstable’ situations. The red arrows indicate vertical motion and the global upward motion. The fire plume is slightly tilted due to forced ventilation (MERCİ; BEJİ, 2016). In this configuration, the Kelvin-Helmholtz instabilities are important.

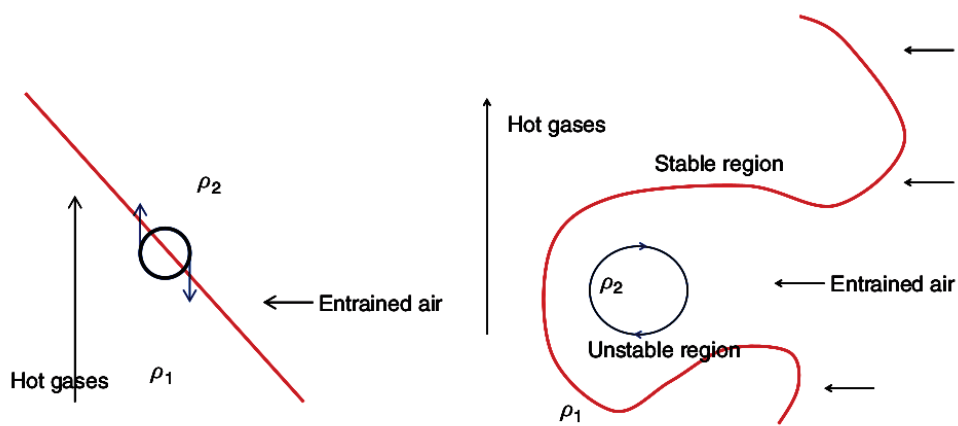
Figure 3 show a zoom of the plume configuration, in which the density difference will provide a substantial contribution in the turbulent flow dynamics of fire plumes.

Figure 2 – Fire plume.



Fonte: (MERCİ; BEJİ, 2016)

Figure 3 – Sketch of: zoom in the flame region, indicating the differences in velocity and density (left); sketch of vortex roll-up with unstable and stable regions (right). Density $\rho_1 < \rho_2$



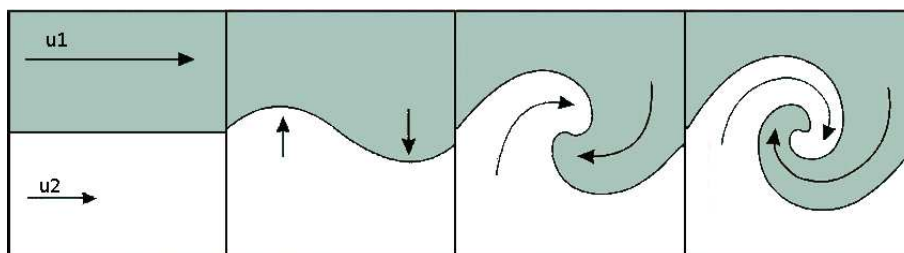
Fonte: (MERCİ; BEJİ, 2016)

In this sense, the simplest configuration to describe the Kelvin-Helmholtz instability is by a reacting mixing layer represented by two parallel reactants streams as different velocity and density.

2.2 Reacting Mixing Layer

Mixing of fuel and oxidizer streams is of primary interest to applications of compressible reacting mixing layers to study Kelvin-Helmholtz instability in the combustion. This configuration is schematically represented in Fig. (4), in which two fluids (fuel and oxidant) of different velocities and densities. When a small disturbance, such as a wave, is introduced at the boundary connecting the fluids, as a consequence, a small velocity perturbation, perpendicular to the shear flow direction, initiates an instability and causes roll up of the shear layers. This phenomenon is known as Kelvin-Helmholtz instability. Thus the processes are controlled by large scale vortical structures (BROWN; ROSHKO, 1974). In the present analysis, the effects of compressibility, heat release and the ratios of density, and velocity are analyzed in the flow structure and what implications this has for the mixing and the consequently heat transfer from the boundaries (system walls).

Figure 4 – Kelvin-Helmholtz instability in shear flow



Fonte: (PAPERIN, 2007).

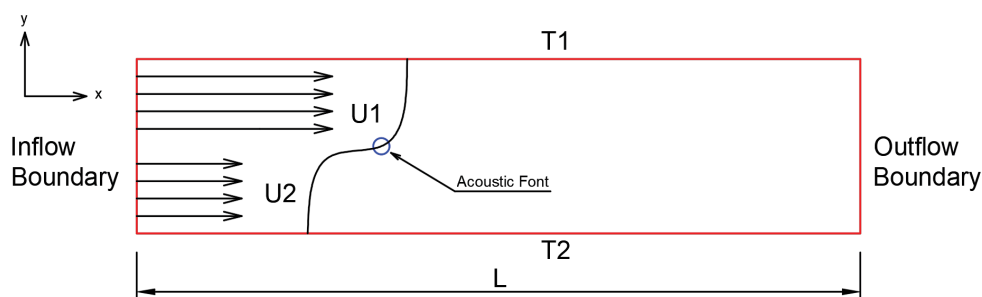
Kelvin-Helmholtz instabilities' growth can also occur in the water. Oceanic and atmospheric sciences study the correlation between mixing effects of the vortices and temperature and salinity in seawater (SMYTH; CARPENTER; LAWRENCE, 2007), (ARMI; FARMER, 1988) or pollution between lakes (ZHU; LAWRENCE, 1996).

3 METHODOLOGY

The stability and acoustic characteristics of binary compressible mixing layer is studied using numerical and analytic methods. The base flow will be obtained through the solution of the axisymmetric boundary layer equations. The stability and acoustic phenomena will be studied through the solution of the stability equations assuming normal mode solutions. The resulting eigenvalue problem posed by the stability equations will be solve both by global methods and shooting methods.

The stability and acoustic problems will also be solved through the direct numerical simulation of the two-dimensional Navier-Stokes equations. High order finite differences will be used in order to reduce dissipation and dispersion errors in the numerical solution. The direct numerical simulation aims at the study of nonlinear effects and non-parallel (spreading of the base flow) effects. The simulation based on two-dimensional set of equations will not allow the study of azimuth modes which will be studied only through the stability equations.

Figure 5 – Problem schematic: mixing layer



Fonte: The author

In the schematic diagram (Figure 5) are represented the inflow velocities, an example of the vertical velocity profile, solution for this initial condition, the boundary conditions for temperature. To stimulate the formation of Kelvin-Helmholtz vortices where used a pressure pulse witch behaves as a gaussian wave and a source in the energy equation. The pressure pulse is is represented in the image in the Rayleigh inflexion point (STRUTT; RAYLEIGH, 1878) to disturb the flow and keep up with the flow response to this disturb.

3.1 Governing Equations

Currie and Currie (2002) explains that from invoking the physical laws of conservation of mass, momentum and energy, this set of equations can be manifested with Lagrangian or Eulerian reference frame employed. In the first the attention is fixed on a particular mass of fluid as it flows with no particles passing through the control volume, while in the second there are particles passing through a control volume fixed in space. The Eulerian reference will be used to derive equations for the conservation laws using cartesian coordinates are used to describe them. (CURRIE; CURRIE, 2002)

The governing equations in compressible form are the non-conservative form of conservation of mass, momentum in horizontal and vertical directions and energy:

$$\frac{\partial \rho^*}{\partial t^*} + \rho^* \frac{\partial u^*}{\partial x^*} + u^* \frac{\partial \rho^*}{\partial x^*} + \rho^* \frac{\partial v^*}{\partial y^*} + v^* \frac{\partial \rho^*}{\partial y^*} = 0 \quad (1)$$

$$\frac{\partial u^*}{\partial t^*} + u^* \frac{\partial u^*}{\partial x^*} + v^* \frac{\partial u^*}{\partial y^*} + \frac{1}{\rho^*} \frac{\partial p^*}{\partial x^*} - \frac{\partial \tau_{xx}^*}{\partial x^*} - \frac{\partial \tau_{xy}^*}{\partial y^*} = 0 \quad (2)$$

$$\frac{\partial v^*}{\partial t^*} + v^* \frac{\partial v^*}{\partial y^*} + u^* \frac{\partial v^*}{\partial x^*} + \frac{1}{\rho^*} \frac{\partial p^*}{\partial y^*} - \frac{\partial \tau_{yy}^*}{\partial y^*} - \frac{\partial \tau_{xy}^*}{\partial x^*} = 0 \quad (3)$$

$$\frac{\partial p^*}{\partial t^*} + u^* \frac{\partial p^*}{\partial x^*} + v^* \frac{\partial p^*}{\partial y^*} + \gamma p^* \frac{\partial u^*}{\partial x^*} + \gamma p^* \frac{\partial v^*}{\partial y^*} - (\gamma - 1) \vec{\tau}^* : \nabla u^* - \nabla \cdot (k^* \nabla T^*) = 0 \quad (4)$$

The energy equation (Eq. 4) was obtained assuming a ideal gas using state equation, the definition of internal energy and the relation between specific heats, specified in Eq. (5). Thus, the internal energy can be written as indicated in Eq. 6.

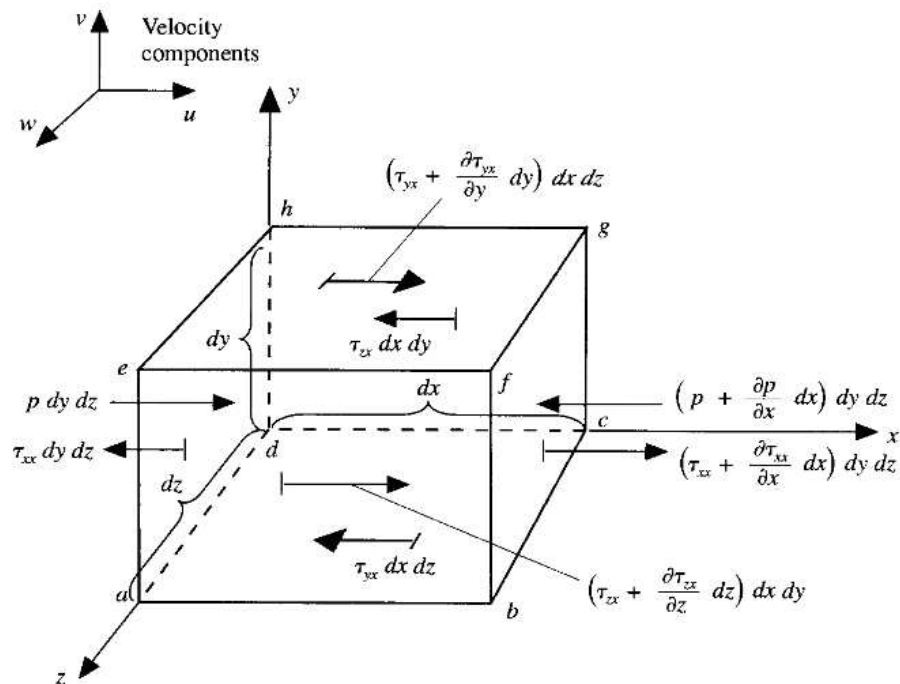
$$p = \rho RT, \quad e = C_v T, \quad \gamma = \frac{C_v}{C_p} \quad (5)$$

$$e = \frac{p}{\rho(\gamma - 1)} \quad (6)$$

3.1.1 Viscosity and thermal conductivity terms

In order for friction between the particles to occur, it must have relative velocity. Relative velocity between adjacent points is responsible for a strain ratio in the fluid element.

Figure 6 – Representation of a fluid element and the forces acting on it's surfaces



Fonte: (ANDERSON, 1995)

Considering the following assumptions for the fluid element:

- isotropic.
- There is no strain when considering rotation, as rotation does not cause relative velocity between particles.
- Linear ratio (Newtonian fluid)
- When there is no motion, $\tau = 0$

The tensor is mathematically represented with:

$$\tau_{ij} = \lambda \frac{\partial u_k}{\partial x_k} \delta_{ij} + \mu \left(\frac{\partial u_i}{\partial x_j} + \frac{\partial u_j}{\partial x_i} \right) \quad (7)$$

The second viscous coefficient, by the Stokes's assumption is:

$$\lambda = -\frac{2}{3}\mu \quad (8)$$

This term is important as the divergent of u is not null. Therefore, the second viscous coefficient must be used in compressible flows. Considering a two-dimensional flow, the strains used are:

$$\tau_{xy} = \mu \left(\frac{\partial u}{\partial y} + \frac{\partial v}{\partial x} \right), \quad \tau_{xx} = \frac{2}{3}\mu \left(2\frac{\partial u}{\partial x} - \frac{\partial v}{\partial y} \right), \quad \tau_{yy} = \frac{2}{3}\mu \left(-\frac{\partial u}{\partial x} + 2\frac{\partial v}{\partial y} \right) \quad (9)$$

The coefficients μ and k , function of temperature, cannot be determined analytically and must be determined empirically. Svehla (1995) disposed values for various chemical species and binaries for NASA Lewis Chemical Equilibrium Program, and are calculated with:

$$\ln(\eta) = A \ln T + \frac{B}{T} + \frac{C}{T^2} + D, \quad \eta = \mu, k \quad (10)$$

The constants A, B, C and D are tabulated coefficients according to each chemical specie. The reference values for temperature T are also tabulated.

3.2 Adimensionalization

The adimensionalization is a technique that removes the physical dimensions from the physical variables by a suitable substitution of variables. This procedure can simplify and parameterize problems where measured units are involved. With the equations expressed in the dimensionless form, the number of variables are reduced and becomes independent of system of unit. The independent non-dimensional variables are defined as

$$x \equiv \frac{x^*}{L_{\text{ref}}}, \quad t \equiv \frac{t^*}{t_{\text{ref}}} = \frac{t^*}{L_{\text{ref}}/a}$$

in which the characteristic time scale t_{ref} is the residence time of a fluid particle with sound speed a in a distance L_{ref} . The non-dimensional dependent variables are defined as

$$T \equiv \frac{T^*}{T_{\text{ref}}}, \quad \rho \equiv \frac{\rho^*}{\rho_{\text{ref}}}, \quad u = \frac{u^*}{a}, \quad v = \frac{v^*}{a}, \quad p = \frac{p^*}{\rho_{\text{ref}} a^2}$$

The transport coefficients in non-dimensional form are

$$\mu \equiv \frac{\mu^*}{\mu_{\text{ref}}}, \quad k \equiv \frac{k^*}{k_{\text{ref}}}$$

in with μ and k are viscosity and thermal conductivity, respectively.

Comparisons between flows with different characteristics may reveal dynamic similarity, and it can be used to development of models to predict properties of the flow or used to simplify mathematical models when some simplification is needed. The Reynolds number (Re) is an adimensional parameter given by $\rho u L / \mu$, that allows to classify the behavior nature of the flow as laminar or turbulent. Is the relation of advective moment terms that tend to turbulence and diffusive terms that tend to stabilize the flow. The Prandtl number (Pr) is an adimensional parameter used in flows when heat transfer occurs. Is the relation of moment difusivity and thermal difusivity and is a fluid property, not a flow property. Once the adimensionalization is done, the Reynolds and Prandtl number reveals the influence of diffusive terms on the flow.

3.2.1 Continuity

The adimensionalization of the continuity equation is given by

$$\left(\frac{\rho_{\text{ref}} a}{L_{\text{ref}}} \right) \frac{\partial \rho}{\partial t} + \left(\frac{\rho_{\text{ref}} a}{L_{\text{ref}}} \right) \frac{\partial \rho u}{\partial x} + \left(\frac{\rho_{\text{ref}} a}{L_{\text{ref}}} \right) \frac{\partial \rho v}{\partial y} = 0 \quad (11)$$

$$\frac{\partial \rho}{\partial t} + \rho \frac{\partial u}{\partial x} + \rho \frac{\partial v}{\partial y} + u \frac{\partial \rho}{\partial x} + v \frac{\partial \rho}{\partial y} = 0 \quad (12)$$

3.2.2 Momentum

The adimensionalization of the momentum equation is given by

$$\left(\frac{\rho_{\text{ref}} a^2}{L_{\text{ref}}}\right) \rho \frac{\partial u}{\partial t} + \left(\frac{\rho_{\text{ref}} a^2}{L_{\text{ref}}}\right) \rho \vec{v} \cdot (\nabla \cdot u) + \left(\frac{\rho_{\text{ref}} a^2}{L_{\text{ref}}}\right) \frac{\partial p}{\partial x} - \left(\frac{\mu_{\text{ref}} a}{L_{\text{ref}}^2}\right) \nabla : \vec{\tau} = 0 \quad (13)$$

$$\frac{\partial u}{\partial t} + u \frac{\partial u}{\partial x} + v \frac{\partial u}{\partial y} + \frac{1}{\rho} \frac{\partial p}{\partial x} - \frac{1}{Re} \left(\frac{\partial \tau_{xx}}{\partial x} + \frac{\partial \tau_{xy}}{\partial y} \right) = 0 \quad (14)$$

$$\frac{\partial v}{\partial t} + v \frac{\partial v}{\partial y} + u \frac{\partial v}{\partial x} + \frac{1}{\rho} \frac{\partial p}{\partial y} - \frac{1}{Re} \left(\frac{\partial \tau_{yy}}{\partial y} + \frac{\partial \tau_{xy}}{\partial x} \right) = 0 \quad (15)$$

3.2.3 Energy

The adimensionalization of the Energy equation is given by

$$\begin{aligned} & \left(\frac{\rho_{\text{ref}} a^3}{L_{\text{ref}}}\right) \frac{\partial p}{\partial t} + \left(\frac{\rho_{\text{ref}} a^3}{L_{\text{ref}}}\right) u \frac{\partial p}{\partial x} + \left(\frac{\rho_{\text{ref}} a^3}{L_{\text{ref}}}\right) v \frac{\partial p}{\partial y} + \left(\frac{\rho_{\text{ref}} a^3}{L_{\text{ref}}}\right) \gamma p \frac{\partial u}{\partial x} \\ & + \left(\frac{\rho_{\text{ref}} a^3}{L_{\text{ref}}}\right) \gamma p \frac{\partial v}{\partial y} - \frac{(\gamma-1) \bar{\mu} \bar{a}^2}{\bar{L}^2} \left(\vec{\tau} : \nabla U \right) - \frac{(\gamma-1) k_{\text{ref}} T_{\text{ref}}}{L_{\text{ref}}^2} \nabla \cdot (k \nabla T) = 0 \end{aligned} \quad (16)$$

$$\frac{\partial p}{\partial t} + u \frac{\partial p}{\partial x} + v \frac{\partial p}{\partial y} + \gamma p \frac{\partial u}{\partial x} + \gamma p \frac{\partial v}{\partial y} - \frac{(\gamma-1)}{Re} \left(\vec{\tau} : \nabla u \right) - \frac{1}{PrRe} \nabla \cdot (k \nabla T) = 0 \quad (17)$$

3.3 Numerical methodology

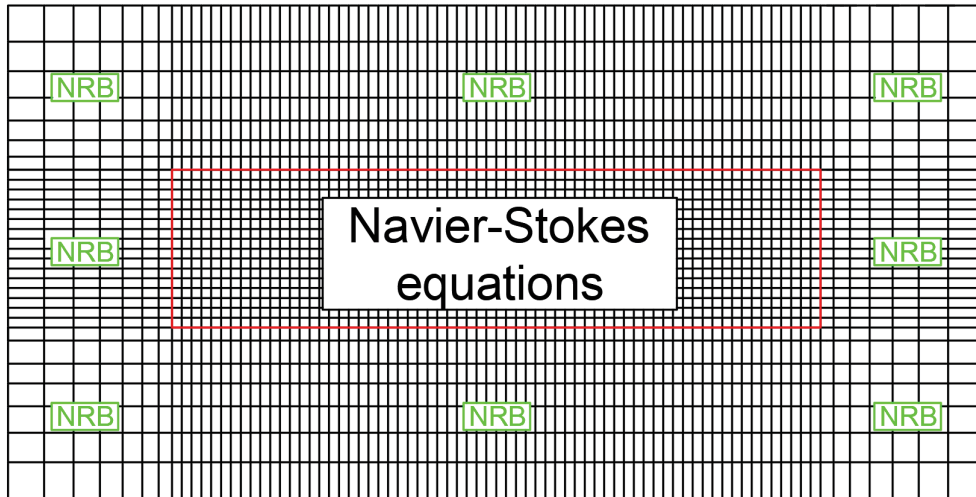
A numerical method capable of capture disturbance evolutions related to hydrodynamic stability, must be of high order, have low dispersion and dissipation properties. Therefore, for spatial and temporal discretization the following schemes are available in the code. (SILVA et al., 2018)

For spatial schemes were used 4th order Central Finite Difference, 6th order Compact Finite Difference (LELE, 1992) and 4th order Dispersion Relation Preserving Finite Difference (TAM; WEBB, 1993) (SILVA et al., 2018).

For temporal schemes were used 4th order, 4 steps Runge Kutta, 4th order, Low

Dissipation and Low Dispersion Runge-Kutta (HU; HUSSAINI; MANTHEY, 1996) and 4th order, Low storage six stage Runge Kutta for non-linear operators (BERLAND; BOGEY; BAILLY, 2006) (SILVA et al., 2018).

Figure 7 – Mesh representation showing interest domain and buffer zone



Fonte: The author

To avoid noise generated at the boundaries from interfere the developing vortices in the domain of interest, non-reflecting boundary conditions are also applied. The figure 7 shows how the computational domain is defined in interest region, where the Navier-Stokes equations are solved and the non-reflecting boundary regions, where the properties are smoothed. More details about the numerical schemes and the boundary condition treatment may be found in (MANCO, 2014).

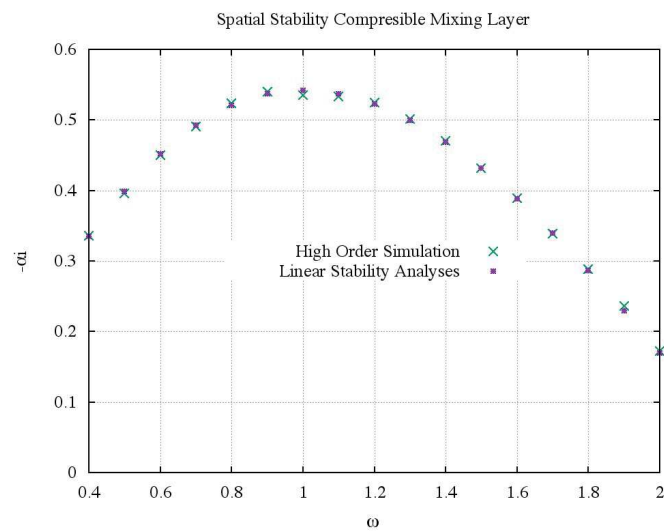
The computational domain used has a 541×481 mesh, resulting in a spacing $\delta x = 0.05$, $\delta y = 0.01$ and $\delta t = 0.01$. It was used a Xeon E5-2609 v3 with 6 cores, with a gcc version 4.8.3. The code has written using Fortran language and Message Passing Interface (MPI) to make parallel computation between 32 cores, resulting in a 40 minutes processing for 80 seconds of flow, for each study case.

3.4 Code Verification

From an code without second-order terms, the present code using Complete Navier-Stokes equations was developed. (SILVA et al., 2018). The numerical scheme

verification was done with a mixing layer where upper and lower streams are equal respectively $U_1 = 0.8$ and $U_2 = 0.2$. Figure 8, taken from (MANCO; MENDONCA, 2018), show a comparison between the growth rate α_i , obtained with kinetic energy along the streamwise direction with a inviscid linear stability analysis code and Euler equations simulations for a several frequencies (SILVA et al., 2018).

Figure 8 – Growth rate versus frequency ω , comparison between linear stability analysis and Euler numerical simulation.



Fonte: Manco and Mendonca (2018)

4 RESULTS AND DISCUSSION

At this reference case will be investigated the effect of temperature gradients with isothermal reference case. Results are presented in terms of flow topology, given by the vorticity, normal velocity and pressure results and also presented in terms of growth rates given by the kinetic energy evolution along the streamwise direction.

4.1 Parameters

The base flow is given by a canonical laminar state defined by the distribution of density, non-dimensional streamwise velocity, and pressure (SILVA et al., 2018). The flow is assumed parallel and the velocity distribution follows a hyperbolic tangent profile. Consider the y axis in equation 18 and 19 the same indicated on figure 5.

$$U(y) = \frac{1}{2} \left[(U_1 + U_2) + (U_1 - U_2) \tanh \left(\frac{2y}{\delta} \right) \right] \quad (18)$$

The upper and lower streams have velocities and temperatures $U_1 = 0.8$, $T_1 = 1$ and $U_2 = .2$, $T_2 = .8$. The mixing thickness $\delta = 0.4$.

The temperature distribution $T(y)$ is given by the Crocco-Busemann relation and the corresponding non-dimensional density is $1/T(y)$. The initial condition used for temperature is: (MANCO, 2014) (SILVA et al., 2018)

$$T(y) = T_1 \frac{y - U_2}{U_1 - U_2} + T_2 \frac{U_1 - y}{U_1 - U_2} + \frac{\gamma - 1}{2} (U_1 - y)(y - U_2) \quad (19)$$

The pressure pulse used as source-term to the energy equation to disturb the flow is: (MANCO, 2014)

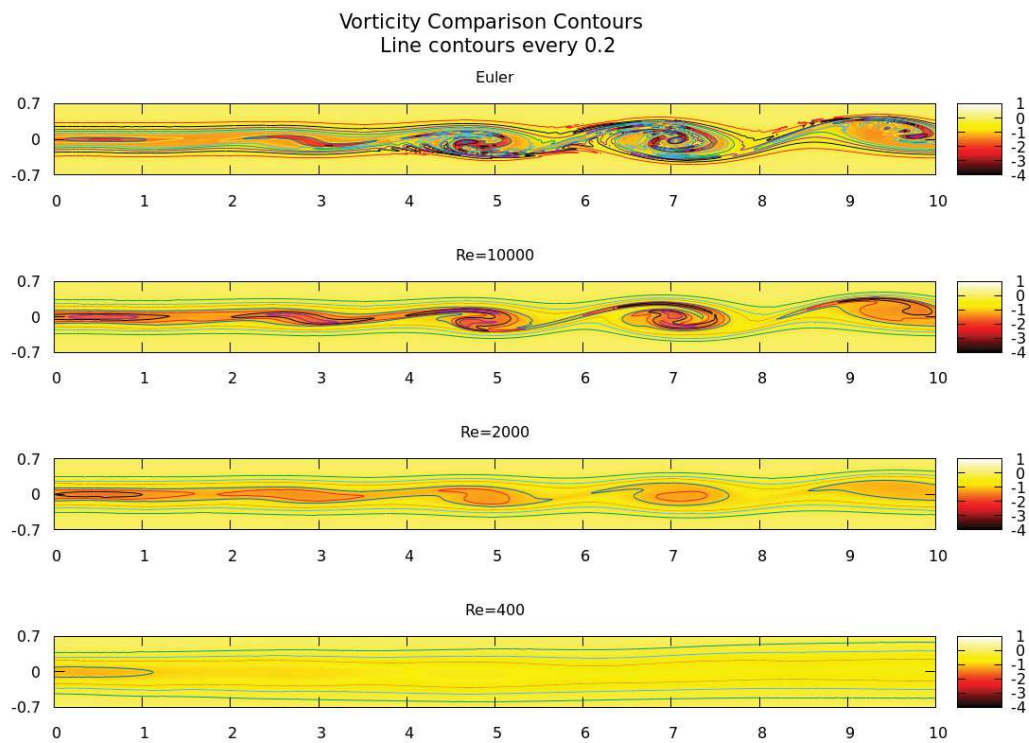
$$s(x, y, t) = a \sin(\omega t) \exp^{-(\ln 2)[(x-x_0)^2 + (y-y_0)^2]/r_0} \quad (20)$$

Where $a = 5$ is the pulse amplitude, $\omega = 1.0$ is the frequency, $x_0 = 0$ and $y_0 = 0$ are the localization in the computational domain and $r_0 = 0.04$ the pulse diameter.

4.2 Reference flow results

Figures 9 through 11 show the evolution of a mixing layer with a temperature gradient with $T_1 = 1$ and $T_2 = 0.8$. The vorticity distributions for the Euler solution (without second-order terms) and Navier-Stokes solution with different Reynolds number are presented in Fig. 9. One expected result from the viscous simulation is the attenuation of noise radiated from the boundaries. The lowest Reynolds number solution show a strong stabilization of the Kelvin-Helmholtz structures due to viscous effects.

Figure 9 – Reference flow vorticity distribution



With the same test case, the figure 10 shows the pressure distribution and the same conclusions are drawn, but the solution is not as noisy as the vorticity, which involve computations of gradients of the velocity field. Finally, the normal velocity field is presented in Fig. 11, where the instability attenuation due to viscous effects are again noticeable.

Figure 10 – Reference flow pressure distribution

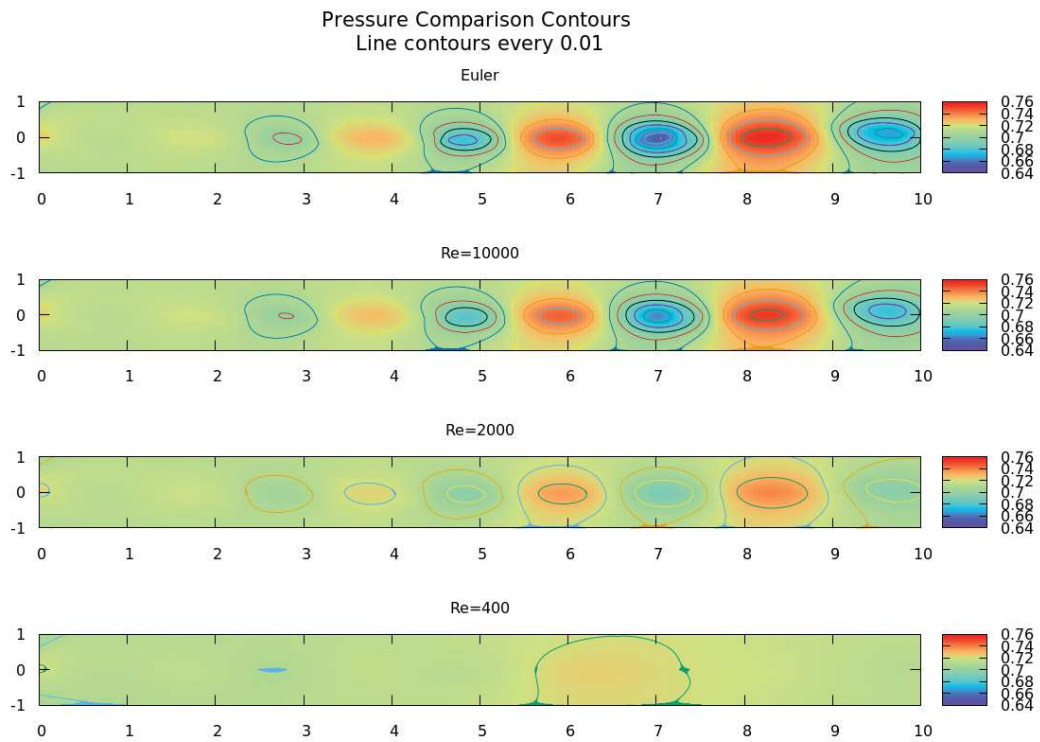
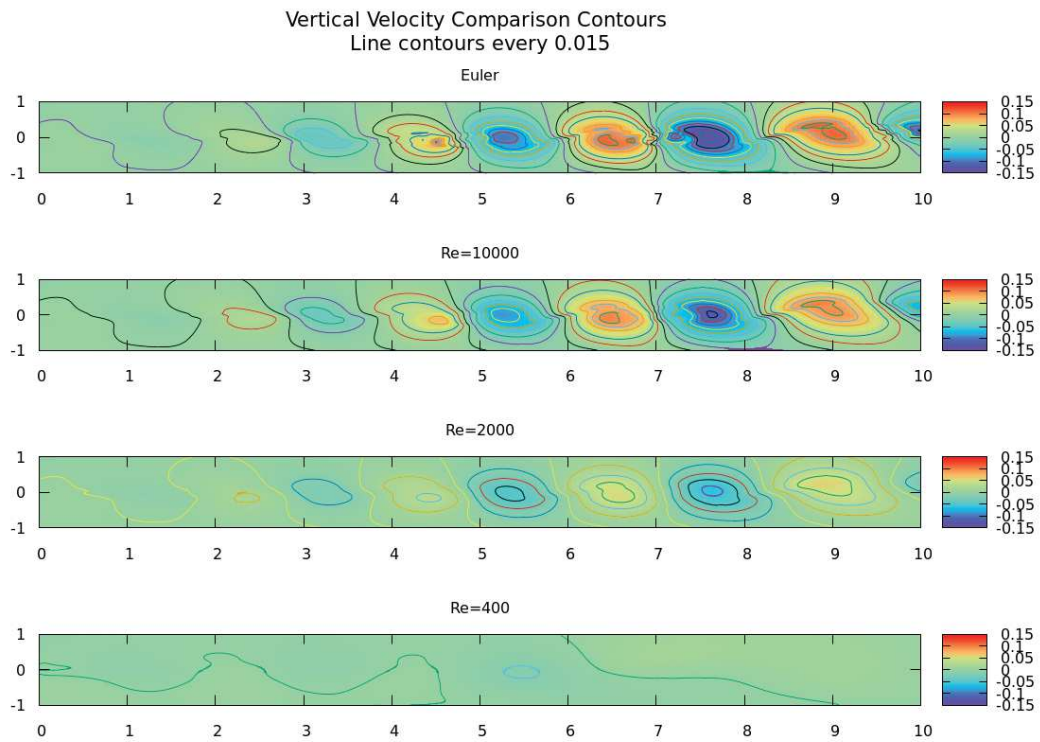


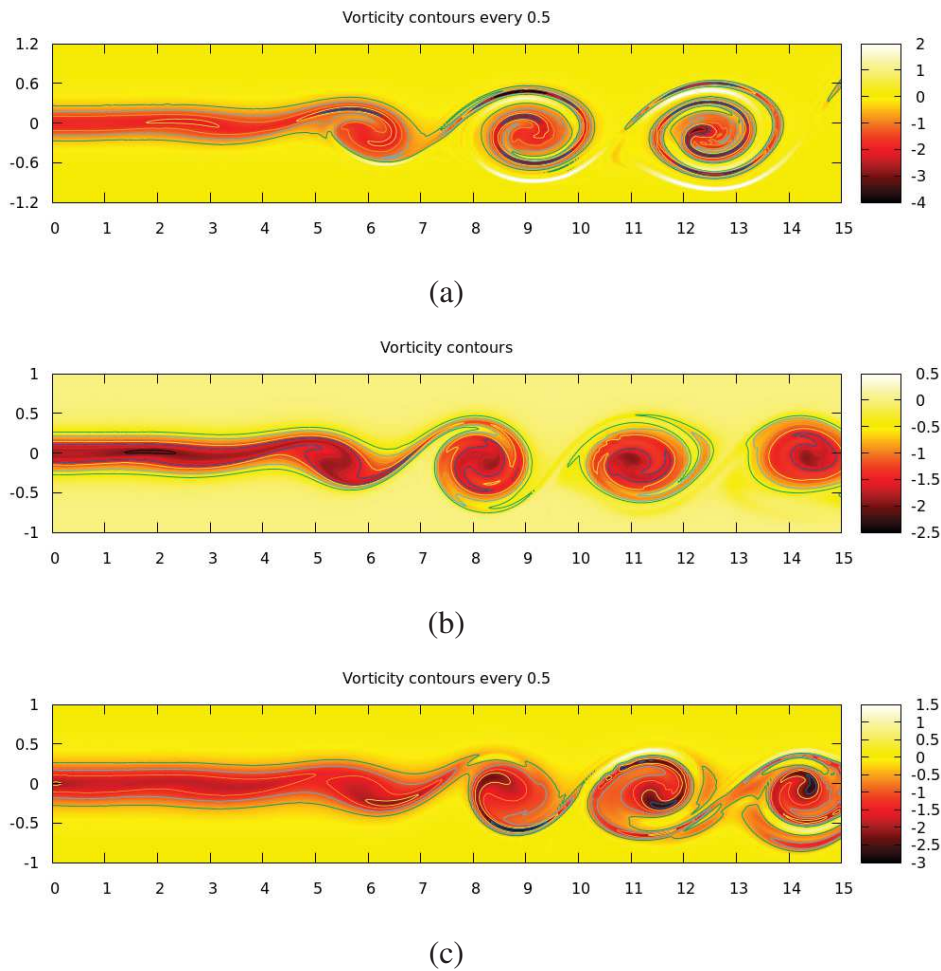
Figure 11 – Reference flow normal velocity component distribution



4.3 Strong Temperature Gradient Cases

In this section is presented the effect of temperature gradients. The upper stream non-dimensional temperature is kept $T_1 = 1$, and the lower stream temperature is fixed at $T_2 = 1$, $T_2 = 0.5$ and $T_2 = 2$. The frequency of each case was selected to correspond to the highest growth rate frequency obtained from a linear stability analysis. For $T_2 = 0.5$ the frequency is $\omega = 0.8$, for $T_2 = 1$, $\omega = 1$ and for $T_2 = 2$, $\omega = 1.2$. Reynolds number used is 10000.

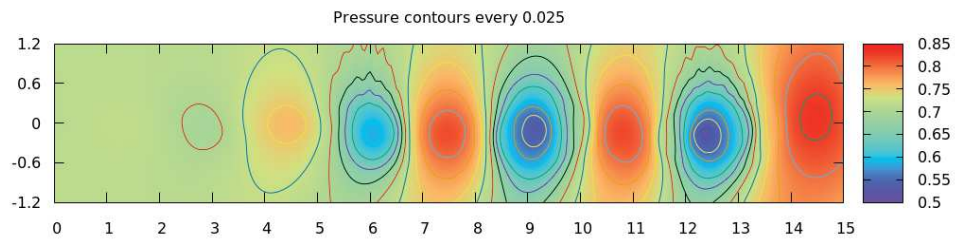
Figure 12 – Vorticity Distribution for $Re=10000$. In figure (a) has values for $T_1 = 1$, $T_2 = 0.5$ and $\omega = 0.8$. Figure (b) has values for $T_1 = 1$, $T_2 = 1$ and $\omega = 1$. Figure (c) has values for $T_1 = 1$, $T_2 = 2$ and $\omega = 1.2$.



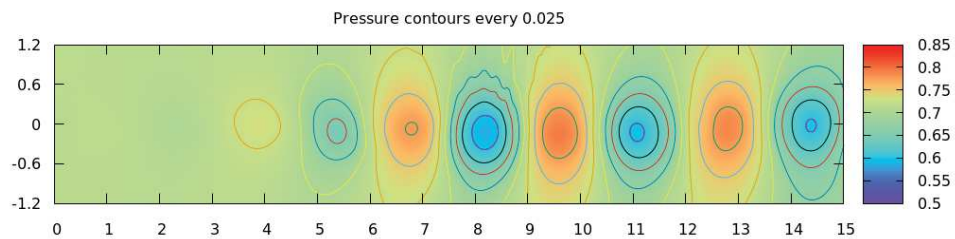
The results are shown in Figs. 9 through 11 in terms of vorticity distribution pressure and normal velocity component. According to Fig. 9, the topology of the flow structure is not significantly affected, but the disturbance growth is stronger for the $T_2 =$

0.5 case, while for $T_2 = 2$ the disturbance is the weakest, as seen in Fig. 13 and 11. These results are consistent with the linear stability analysis presented in the next section. The wave-number change due to changes in T_2 is also consistent with the linear stability results, where one has to observe that each case correspond to a different frequency.

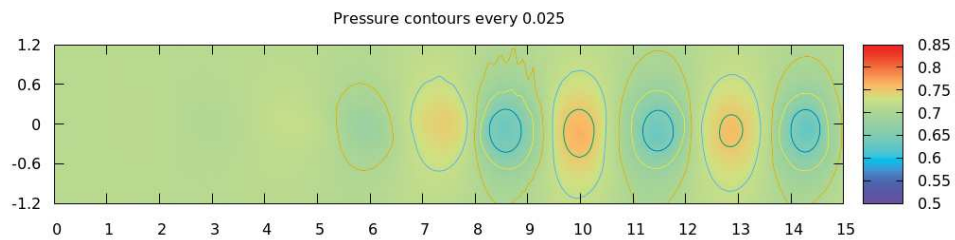
Figure 13 – Pressure distribution for $Re=10000$. The figure (a) has values for $T_1 = 1$ and $T_2 = 0.5$, $\omega = 0.8$. Figure (b) has values for $T_1 = 1$ and $T_2 = 1$, $\omega = 1$ and figure (c) $T_1 = 1$ and $T_2 = 2$, $\omega = 1.2$.



(a)

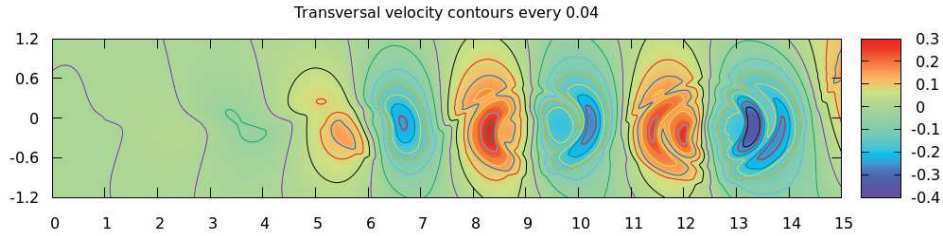


(b)

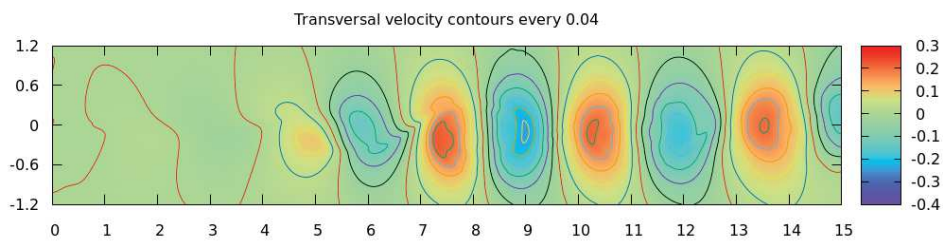


(c)

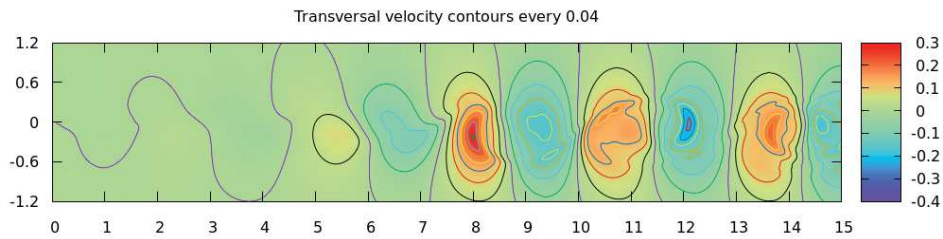
Figure 14 – Normal velocity component for $Re=10000$. Figure (a) has values for $T_1 = 1$ and $T_2 = 0.5$, $\omega = 0.8$. Figure (b) has values for $T_1 = 1$ and $T_2 = 1$, $\omega = 1$ and figure (c) has values for $T_1 = 1$ and $T_2 = 2$, $\omega = 1.2$.



(a)



(b)



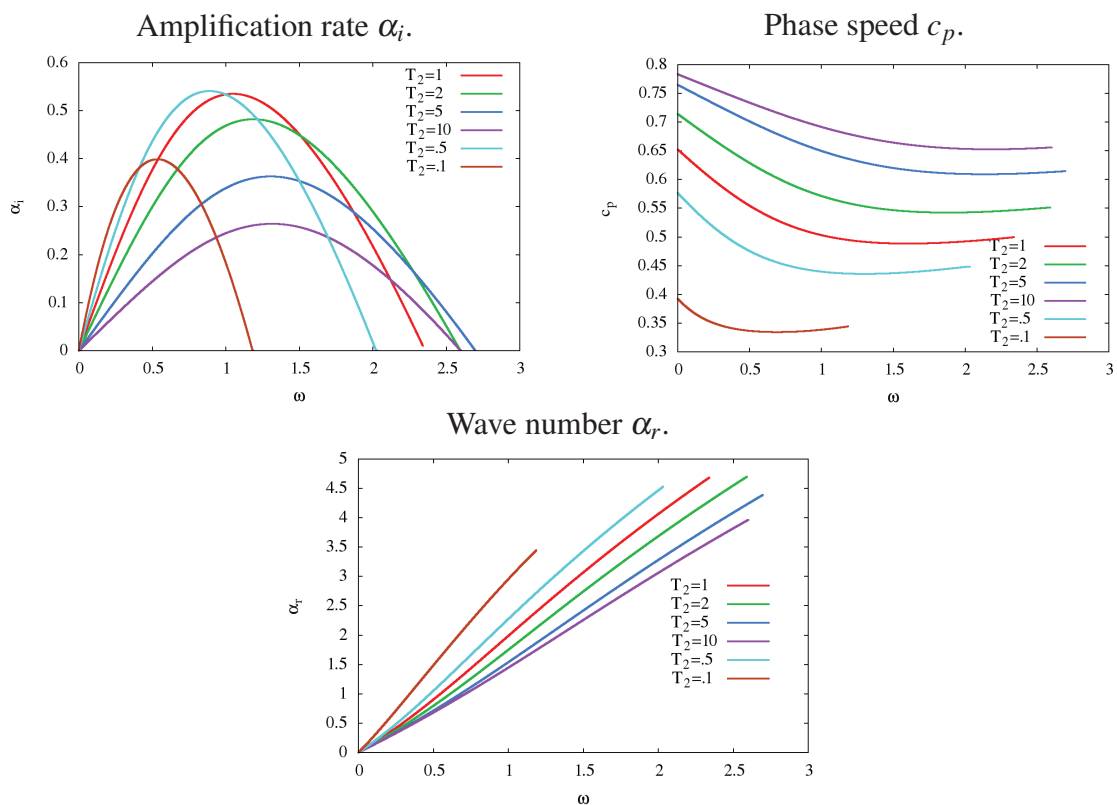
(c)

4.4 Linear Stability Theory Analysis

Figure 15 shows the growth rate, phase speed and wavenumber for lower stream temperature T_2 from 0.1 to 10 obtained varying the frequency ω from 0 to 3, calculating the kinetic energy and applying the Fast Fourier Transform (FFT) to obtain them. The results show that as lower is the stream temperature, smaller is the range of unstable frequencies. The growing mode for $T_2 = 0.5$ is larger than that for the isothermal case. As the slow stream temperature is decreased the flow becomes more stable, both in terms of the highest amplification rate and in terms of the range of unstable frequencies. For higher slow stream temperature, the mixing layer becomes more stable, but the range of unstable frequencies increase with increasing T_2 . The phase speed increases as the lower stream

temperature is increased while the wavenumber reduces monotonically. The wavenumber observed in the DNS solutions are compatible with this results, considering that each case was run at a different frequency, the one corresponding to the highest amplification rate. As T_2 is increased, the frequency considered is reduced, resulting in a lower wavenumber for the lower T_2 and a higher wavenumber for the higher T_2 . Nevertheless the dispersion characteristic, with a relatively constant phase speed with frequency, does not change with T_2 , where the results show that the phase speed levels off for higher frequencies. (SILVA et al., 2018)

Figure 15 – Linear Stability Theory results. Effect of Temperature gradient. $T_1 = 1$ through $T_2 = 0.1$ to 10 using $Re=10000$.



5 CONCLUSIONS

This work contributed to the understanding of the development and evolution of hydrodynamic instabilities. Results with linear stability theory with respect to wavenumber, wave speed amplification rate are consistent with the the solution obtained with direct numerical simulation using low dispersion and dissipation and high order method. Was observed different amplification rate for different temperature gradients, where higher temperature T_2 decreases the rate but and lower temperatures can increase the amplification and decrease the spectrum of frequencies that can amplify the disturbance. About the phase speed c_p of the disturbance, is observed higher values as the temperature increases and lower values when T_2 decreases. The wave number, inversely proportional to the wave-length, and assuming the disturbance propagates as a Gaussian, has higher values as T_2 decreases for the same frequency ω . The results with different Reynolds number confirmed the stable behavior expected to the flow for low Reynolds numbers.

This work also tried to make advances in studies of combustion and hydrodynamic instabilities. So far, only the mixing layer without chemical reaction has been analyzed. In this case the problem was solved by the following governing equations: mass, momentum in the x and y directions, energy and state equation. For the chemical reaction of the flame to be implemented it is necessary to include conservation equations of reactants (fuel and oxidant). However, due to the difficulty of solving the chemical reaction term present in the species and energy equations, the Zel'dovich procedure will be used. This method eliminates the source of the chemical reaction of the equations by combining the governing equations. Thus the solution is obtained through new conservative variables: mixture fraction and excess enthalpy. For more details, the formulation is present on Appendix A.

REFERENCES

- ABADI, M.; LEINO, K. R. M. A logic of object-oriented programs. In: **Theory and Practice of Software Development, TAPSOFT**. [S.l.]: Berlin: Springer-Verlag, 1997. (Lecture Notes in Computer Science, v. 1214), p. 682–696.
- ANDERSON, J. **Computational Fluid Dynamics: The Basics with Applications**. [S.l.]: McGraw-Hill, 1995. (McGraw-Hill International Editions: Mechanical Engineering). ISBN 9780071132107.
- ARMI, L.; FARMER, D. M. The flow of mediterranean water through the strait of gibraltar. the flow of atlantic water through the strait of gibraltar. **Progress in Oceanography**, v. 21, n. 1, p. 1–105, 1988.
- BERLAND, J.; BOGEY, C.; BAILLY, C. Low-dissipation and low-dispersion fourth-order runge–kutta algorithm. **Computers & Fluids**, Elsevier, v. 35, n. 10, p. 1459–1463, 2006.
- BROWN, G. L.; ROSHKO, A. On density effects and large structure in turbulent mixing layers. **Journal of Fluid Mechanics**, Cambridge University Press, v. 64, n. 4, p. 775–816, 1974.
- CURRIE, I. G.; CURRIE, I. **Fundamental mechanics of fluids**. [S.l.]: Crc Press, 2002.
- FERNANDES, L. M.; FREITAS, R. B.; MENDONCA, M. T. Stability of o₂/h₂ binary mixing layers: Effect of temperature gradients, compressibility and three-dimensionality. In: **IX Escola de Primavera de Transição e Turbulência**. São Leopoldo, RS: [s.n.], 2014. p. 1–10.
- FREITAS, R. B.; FERNANDES, L. M.; MENDONCA, M. T. Three-dimensional disturbances on binary mixing layers modified by jets and wakes. In: **IUTAM Symp. on Laminar-Turbulent Transition**. Rio de Janeiro, Brazil: [s.n.], 2014. Accepted for presentation.
- HU, F. Q.; HUSSAINI, M. Y.; MANTHEY, J. L. Low-dissipation and low-dispersion runge–kutta schemes for computational acoustics. **Journal of Computational Physics**, Elsevier, v. 124, n. 1, p. 177–191, 1996.
- LELE, S. K. Compact finite difference schemes with spectral-like resolution. **Journal of computational physics**, Elsevier, v. 103, n. 1, p. 16–42, 1992.
- MANCO, J. A. A. **Non-reflecting boundary conditions for high order numerical simulation of compressible Kelvin-Helmholtz instability**. 131 p. Dissertation (Master's Degree in Spatial Engineering and Technology) — Instituto Nacional de Pesquisas Espaciais (INPE), São José dos Campos, 2014. INPE-17465-TDI/2256.
- MANCO, J. A. A.; MENDONCA, M. T. Direct numerical simulation of binary free shear layer hydrodynamic stability. In: **IUTAM Symp. on Laminar-Turbulent Transition**. Rio de Janeiro, Brazil: [s.n.], 2014. Accepted for presentation.
- MANCO, J. A. A.; MENDONCA, M. T. Comparative study of different non-reflecting boundary conditions for compressible flows. **Computer and Fluids, Submitted for Publication**, v. 0, p. 0, 2018.

MENDONÇA, M. T. Cooled gas turbine blade trailing edge flow analysis. In: **13th Brazilian Congress of Engineering and Thermal Sciences - ENCIT 2010**. Uberlândia - MG, Brazil: [s.n.], 2010. p. 1–9.

MENDONCA, M. T. Linear stability analysis of binary compressible mixing layers modified by a jet or a wake deficit. In: **52nd AIAA Aerospace Sciences Meeting and Exhibit**. National Harbor, Maryland: [s.n.], 2014. p. 1–13.

MERCI, B.; BEJI, T. **Fluid mechanics aspects of fire and smoke dynamics in enclosures**. [S.l.]: CRC/Balkema, Taylor & Francis Group, 2016. 364 p. ISBN 978-1-138-02960-6.

PAPERIN, M. **Kelvin-Helmholtz Instability Cloud Structure**. 2007. <<https://www.brockmann-consult.de/CloudStructures/kelvin-helmholtz-instability-description.htm>>. Accessed in: 30 Nov. 2018.

QUIRINO, S. F. **Simulação numérica direta de camada cisalhante compressível com fonte de calor**. 103 p. Dissertation (Dissertação (Mestrado em Engenharia e Tecnologia Espaciais)) — Instituto Nacional de Pesquisas Espaciais (INPE), São José dos Campos, 2006. (INPE-14661-TDI/1217).

SALEMI, L.; MENDONCA, M. T. Spatial and temporal linear stability analysis of binary compressible shear layer. In: **AIAA 38th Fluid Dynamics Conference**. Seattle, USA: [s.n.], 2008. (AIAA paper 2008-3841), p. 1–23.

SALEMI, L. C. **Análise de Estabilidade Linear de Camada de Mistura Compressível Binária**. 216 p. Dissertation (Dissertação (Mestrado em Engenharia e Tecnologia Espaciais)) — Instituto Nacional de Pesquisas Espaciais (INPE), São José dos Campos, 2006.

SILVA, M. et al. Mixing layer stability analysis with strong temperature gradients. In: . [S.l.: s.n.], 2018.

SMYTH, W.; CARPENTER, J.; LAWRENCE, G. Mixing in symmetric holmboe waves. **Journal of physical oceanography**, v. 37, n. 6, p. 1566–1583, 2007.

SOARES, M. S.; FILHO, F. F.; MENDONCA, M. T. Effect of thickness ratio on the stability of mixing layers with a wake component. In: **IX Escola de Primavera de Transição e Turbulência**. São Leopoldo, RS: [s.n.], 2014. p. 1–7.

SOUZA, O. M. R. **Análise de Instabilidades Lineares em Camadas de Mistura Planas Duplas e Compressíveis**. 67 p. Dissertation (Dissertação) — Instituto Militar de Engenharia - IME, Rio de Janeiro, 2011.

SOUZA, O. M. R.; ALVES, L. S. B.; MENDONCA, M. T. Double mixing layer linear stability analysis. In: **IX Escola de Primavera de Transição e Turbulência**. São Leopoldo, RS: [s.n.], 2014. p. 1–8.

STRUTT, J. W.; RAYLEIGH, L. On the instability of jets. **Proc. London Math. Soc.**, v. 10, n. 4, 1878.

SVEHLA, R. A. Transport coefficients for the nasa lewis chemical equilibrium program. 1995.

TAM, C. K. W.; WEBB, J. C. Dispersion-relation-preserving schemes for computational acoustics. **Journal of Computational Physics**, v. 107, n. 184, p. 262–281, September 1993.

ZHU, Z.; LAWRENCE, G. A. Echange flow through a channel with an underwater sill. **Dynamics of atmospheres and oceans**, Elsevier, v. 24, n. 1-4, p. 153–161, 1996.

APPENDIX A — SHVAB-ZEL'DOVICH FORMULATION FOR DIFFUSION FLAMES

A.1 Conservation of species equation

Considering the chemical specie i , with specific mass ρ_i , the mass fraction Y_i is defined as:

$$Y_i = \frac{\rho_i}{\rho} \quad (21)$$

The species conservation equation in a volume V , in an eulerian reference system can be expressed as the accumulation of the property inside the volume, summed with the property increment through the area A that involves the volume V , and, using Gauss's Theorem, the area integral is transformed in a volume integral:

$$\frac{d}{dt} \int_V \rho Y_i dV = \int_V \frac{\partial \rho Y_i}{\partial t} dV + \int_A \rho Y_i (\vec{v} \cdot \vec{n}) dA = - \int_A \vec{Q}_i \cdot \vec{n} dA + \int_V \rho \omega_i dV \quad (22)$$

$$\int_V \frac{\partial \rho Y_i}{\partial t} dV + \int_V \nabla \cdot (\rho \vec{V} Y_i) dV = - \int_V \nabla \cdot \vec{Q}_i dV + s_i \int_V \rho \omega dV \quad (23)$$

$$\frac{\partial \rho Y_i}{\partial t} + \nabla \cdot (\rho \vec{V} Y_i) = - \nabla \cdot \vec{Q}_i + s_i \rho \omega \quad (24)$$

Where the terms on the right-hand side represent the mass diffusion and the rate of chemical reaction.

The chemical reaction term w is:

$$w = B Y_O Y_F e^{E/RT} \quad (25)$$

Where B represents the collisions between the oxidizer O and fuel F molecules, and the effectiveness of the collisions is defined as $e^{-E/RT}$, where E is the energy activation. Thus, the conservation of species equation in the non-conservative form becomes:

$$\rho \left[\frac{\partial}{\partial t} Y_i + \vec{v} \cdot \nabla Y_i \right] = \nabla \cdot (\rho D_i \nabla Y_i) - \rho \omega_i \quad (26)$$

A.2 Energy equation with reactive terms

From the internal energy equation for a reactive flow:

$$\frac{\partial \rho e}{\partial t} + \nabla \cdot \rho \vec{v} e = -p \cdot \nabla \vec{v} + \vec{\tau} : \nabla \vec{v} + \nabla \cdot (k \nabla T) + \nabla \cdot (\rho D_i \nabla Y_i) h_i \quad (27)$$

From the of internal energy, $e = h - p/\rho$, re-writing:

$$\frac{\partial \rho (h - p/\rho)}{\partial t} + \nabla \cdot \rho \vec{v} \left(h - \frac{p}{\rho} \right) = -p \nabla \cdot \vec{v} + \vec{\tau} : \nabla \vec{v} + \nabla \cdot (k \nabla T) + \nabla \cdot (\rho D_i \nabla Y_i h_i) \quad (28)$$

Expanding the equation 28:

$$\frac{\partial \rho h}{\partial t} + \nabla \cdot \rho \vec{v} h - \frac{\partial p}{\partial t} - \nabla \cdot p \vec{v} = -p \nabla \cdot \vec{v} + \vec{\tau} : \nabla \vec{v} + \nabla \cdot (k \nabla T) + \nabla \cdot (\rho D_i \nabla Y_i h_i) \quad (29)$$

Using the chain rule for the forth term:

$$\frac{\partial \rho h}{\partial t} + \nabla \cdot \rho \vec{v} h - \frac{\partial p}{\partial t} - \vec{v} \cdot \nabla p = \vec{\tau} : \nabla \vec{v} + \nabla \cdot (k \nabla T) + \nabla \cdot (\rho D_i \nabla Y_i h_i) \quad (30)$$

From the definition of enthalpy:

$$h = \sum_i Y_i (h_i^0 + h_i^T) = Y_i \hat{h}_i^0 + \hat{h} \quad (31)$$

Considering that there is a local thermodynamic balance,

$$Y_i \hat{h}_i^0 \equiv \sum_i Y_i h_i^0, \quad \hat{h} \equiv \sum_i Y_i h_i^T = \sum_i Y_i \int_{T_{ref}}^T c_{p_i} dT$$

Re-writing:

$$\begin{aligned} \frac{\partial \rho (Y_i \hat{h}_i^0)}{\partial t} + \nabla \cdot (\rho \vec{v} Y_i \hat{h}_i^0) + \frac{\partial \rho \hat{h}}{\partial t} + \nabla \cdot (\rho \vec{v} \hat{h}) - \frac{\partial p}{\partial t} - \vec{v} \cdot \nabla p = \\ \vec{\tau} : \nabla u + \nabla \cdot (k \nabla T) + \nabla \cdot [\rho D_i \nabla Y_i (h_i^0 + h_i^T)] \end{aligned} \quad (32)$$

After regroup the terms:

$$\sum_i \bar{h}_i^0 \left[\frac{\partial \rho Y_i}{\partial t} + \nabla \cdot (\rho \vec{v} Y_i) - \nabla \cdot (\rho D_i \nabla Y_i) \right] = \sum_i \bar{h}_i^0 (\rho \omega_i) \quad (33)$$

As term in the equation 34 is not expressive for the flow, a simplification is done with:

$$\nabla \cdot \sum_i (\rho D_i \nabla Y_i \bar{h}_i^T) = 0 \quad (34)$$

For simplicity and for initial validation of code, the specific heat is considered constant:

$$\bar{h} = \int_{T_0}^T c_p dT = c_p \int_{T_0}^T dT = c_p T \quad (35)$$

With the definitions above the chemical reaction can be insert in the system of equations, witch, in the non-conservative form becomes:

$$\rho \left[\frac{\partial c_p T}{\partial t} + \vec{v} \cdot \nabla (c_p T) \right] - \frac{\partial p}{\partial t} + \vec{v} \cdot \nabla p - \vec{\tau} : \nabla \vec{v} - \nabla \cdot (k \nabla T) = Q \rho \omega \quad (36)$$

Where the terms, respectively, represents the energy accumulation, convective transport, time pressure rate, pressure gradient, viscous dissipation, heat transfer due the convection, heat transfer due the diffusion and the chemical reaction time rate.

Different from the equation 4, where the primitive variable is the pressure, is demonstrated below, where changed to use temperature due the pressure Diferentente da formulação adotada inicialmente que usava a equação da energia em termos de pressão, como será visto adiante, esta foi alterada para termos de temperatura due to the symmetry of the operators, thus, simplifying the complexity of the formulation.

A.3 Adimensionalization

The independent non-dimensional variables are defined as:

$$x \equiv \frac{\hat{x}}{\hat{L}_c}, \quad t \equiv \frac{\hat{t}}{\hat{t}_c} = \frac{\hat{t}}{\hat{L}_c / \hat{a}}$$

Where the characteristic time scale \hat{t}_c is the residence time of a fluid particle with velocity \hat{a} in a distance \hat{L} .

The dependent non-dimensional variables are defined as:

$$\rho \equiv \frac{\hat{\rho}}{\hat{\rho}_c}, \quad v_i = \frac{\hat{v}_i}{\hat{v}_c}, \quad p = \frac{\hat{p}}{\hat{\rho}_c \hat{v}_c^2}, \quad i=1, 2, 3$$

In this analysis, the characteristic velocity \hat{v}_c is the sound velocity with characteristic temperature \hat{T}_c , $\hat{v}_c = \hat{a}_c = (\gamma R \hat{T}_c)^{1/2}$. The transport coefficients in the non-dimensional form are:

$$\mu \equiv \frac{\hat{\mu}}{\hat{\mu}_c}, \quad k \equiv \frac{\hat{k}}{\hat{k}_c}, \quad D_n \equiv \frac{\hat{D}_n}{\hat{D}_{nc}}, \quad n=F, O$$

A.3.1 Energy equation with chemical reaction

From the dimensional form:

$$\rho \left[\frac{\partial \hat{c}_p \hat{T}}{\partial \hat{t}} + \vec{v} \cdot \nabla (\hat{c}_p \hat{T}) \right] - \frac{\partial \hat{p}}{\partial \hat{t}} + \vec{v} \cdot \nabla \hat{p} - \vec{\tau} : \nabla \hat{v} - \nabla \cdot (\hat{k} \nabla \hat{T}) = Q \hat{\rho} \omega \quad (37)$$

Defining $\hat{\nabla} = (1/\hat{L}_c) \nabla$, the magnitude order of each term is described below:

$$\frac{\hat{\rho}_c \hat{c}_p \hat{T}_c}{\hat{t}_c}, \quad \frac{\hat{\rho}_c \hat{c}_p \hat{T}_c \hat{v}_c}{\hat{L}_c}, \quad \frac{\hat{\rho}_c \gamma R \hat{T}_c}{\hat{t}_c}, \quad \frac{\hat{v}_c \hat{\rho}_c \gamma R \hat{T}_c}{\hat{L}_c}, \quad \frac{\hat{\mu}_c \hat{v}_c \hat{v}_c}{\hat{L}_c \hat{L}_c}, \quad \frac{\hat{k}_c \hat{T}_c}{\hat{L}_c^2}, \quad Q \hat{\rho}_c B \quad (38)$$

Dividing by $\hat{\rho}_c \hat{c}_p \hat{T}_c$ and after by \hat{v}_c / \hat{L}_c ($\hat{t}_{res} \equiv \hat{L}_c / \hat{v}_c$):

$$\frac{\hat{t}_{res}}{\hat{t}_c}, \quad 1, \quad \frac{\hat{t}}{\hat{t}_c} \frac{\gamma R}{\hat{c}_p}, \quad \frac{\gamma R}{\hat{c}_p}, \quad \frac{\hat{\mu}_c \hat{v}_c^2}{\hat{L}_c \hat{\rho}_c \hat{v}_c c_p \hat{T}_c}, \quad \frac{\hat{k}_c}{\hat{v}_c \hat{L}_c \hat{\rho}_c c_p}, \quad \frac{Q}{\hat{c}_p \hat{T}_c} \frac{B \hat{L}_c}{\hat{v}_c} \quad (39)$$

Since that $St = \hat{t}_{res} / \hat{t}_c$, $(\gamma - 1) = \gamma R / \hat{c}_p$, $\hat{v} = \hat{\mu}_c / \hat{\rho}_c$, $\alpha = \hat{k} / \hat{\rho}_c c_p$, $1/Pe = \alpha / \hat{u} \hat{L}$, $Da = \hat{L}_c B / \hat{v}_c$, and $\hat{v}_c^2 = \gamma R \hat{T}_c$.

$$St, \quad 1, \quad St(\gamma - 1), \quad (\gamma - 1), \quad \frac{\gamma - 1}{Re}, \quad \frac{1}{Pe}, \quad qDa \quad (40)$$

Defining $\omega = Da Y_O^n Y_F^n e^{-\beta/T}$, the non-dimensional form is:

$$\rho \left[St \frac{\partial T}{\partial t} + \vec{v} \cdot \nabla T \right] - (\gamma - 1) \left[St \frac{\partial p}{\partial t} + \vec{v} \cdot \nabla p \right] =$$

$$\left(\frac{\gamma - 1}{Re} \right) \vec{\tau} : \nabla \vec{v} + \frac{1}{Pe} \nabla \cdot (k \nabla T) + q \rho \omega \quad (41)$$

A.3.2 Chemical Species

$$\rho \left[\frac{\partial}{\partial \hat{t}} \hat{Y}_i + \vec{v} \cdot \nabla \hat{Y}_i \right] = \nabla \cdot (\hat{\rho} \hat{D}_i \nabla \hat{Y}_i) + s_i \hat{\rho} \omega \quad (42)$$

The magnitude order of each term is demonstrated below:

$$\frac{\hat{\rho}_c \hat{Y}_c}{\hat{t}_c}, \quad \frac{\hat{\rho} \hat{v} \hat{Y}_c}{\hat{L}_c}, \quad \frac{\hat{\rho} \alpha_c \hat{Y}_c}{\hat{L}_c^2}, \quad \hat{\rho}_c B \hat{Y}_{Fc} \hat{Y}_{Oc} \quad (43)$$

For Lewis $Le = 1$, $D_O = D_F = \alpha$ and dividing by $\hat{\rho}_c \hat{v}_c \hat{Y}_c / \hat{L}_c$:

$$St, \quad 1, \quad \frac{1}{Pe}, \quad Da \quad (44)$$

In the non-conservative form:

$$St \rho \frac{\partial}{\partial t} Y_i + \rho \vec{v} \cdot \nabla Y_i = \frac{1}{Pe} \nabla \cdot (\rho \alpha \nabla Y_i) - S_i \rho \omega \quad (45)$$

in which $S_O = S = s_O \hat{Y}_{Fc} / \hat{Y}_{Oc}$ e $S_F = 1$.

A.4 Eliminating the chemical reaction from the energy equation

The Zeldovich formulation allows to adopt an infinitely narrow region of the flame, and in this interface all the fuel reacts with the oxidizer. This allows to eliminate the exponential term, highly non-linear, present in the energy equation.

$$St \rho \frac{\partial T}{\partial t} + \rho \vec{v} \cdot \nabla T - (\gamma - 1) \left[St \frac{\partial p}{\partial t} + \vec{v} \cdot \nabla p \right] - \left(\frac{\gamma - 1}{Re} \right) \vec{\tau} : \nabla u - \frac{1}{Pe} \nabla \cdot (k \nabla T) = q \rho \omega \quad (46)$$

Defining $p = \rho T$, $D\rho/Dt = -\rho\nabla \cdot \vec{v}$ and reordering the terms:

$$St\rho \frac{\partial T}{\partial t} + \rho\vec{v} \cdot \nabla T - (\gamma - 1) \left[St \left(\rho \frac{\partial T}{\partial t} + \rho\vec{v} \cdot \nabla T \right) - \rho T (\nabla \cdot \vec{v}) \right] - \left(\frac{\gamma - 1}{Re} \right) \vec{\tau} : \nabla u - \frac{\nabla}{Pe} \cdot (k\nabla T) = q\rho\omega \quad (47)$$

Expanding the third term:

$$(2 - \gamma) \left[St\rho \frac{\partial T}{\partial t} + \rho\vec{v} \cdot \nabla T \right] = -(\gamma - 1)\rho T \nabla \cdot \vec{v} + \left(\frac{\gamma - 1}{Re} \right) \vec{\tau} : \nabla v + \frac{\nabla}{Pe} \cdot (k\nabla T) + q\rho\omega \quad (48)$$

With the following manipulation:

$$\begin{aligned} & \frac{1}{Pe} \nabla \cdot [\rho\alpha \nabla (T + (2 - \gamma)T - (2 - \gamma)T)] = \\ & \frac{1}{Pe} \nabla \cdot [\rho\alpha \nabla ((2 - \gamma)T)] + \frac{1}{Pe} \nabla \cdot [\rho\alpha \nabla (T(\gamma - 1))] \end{aligned}$$

Is possible to re-write the equation 48 as:

$$\begin{aligned} (2 - \gamma) \left[St\rho \frac{\partial T}{\partial t} + \rho\vec{v} \cdot \nabla T \right] &= (2 - \gamma) \frac{1}{Pe} \nabla \cdot (\rho\alpha \nabla T) + \\ & (\gamma - 1) \frac{1}{Pe} \nabla \cdot (\rho\alpha \nabla T) + \left(\frac{\gamma - 1}{Re} \right) \vec{\tau} : \nabla \vec{v} - (\gamma - 1)\rho T \nabla \cdot \vec{v} + q\rho\omega \quad (49) \end{aligned}$$

With the chemical species, the equations are:

$$St\rho \frac{\partial}{\partial t} Y_O + \rho\vec{v} \cdot \nabla Y_O = \frac{1}{Pe} \nabla \cdot (\rho\alpha \nabla Y_O) - S\rho\omega \quad (50)$$

From definition $s_F = 1$

$$St\rho \frac{\partial}{\partial t} Y_F + \rho\vec{v} \cdot \nabla Y_F = \frac{1}{Pe} \nabla \cdot (\rho\alpha \nabla Y_F) - \rho\omega \quad (51)$$

Multiplying the equation (49) $\times (S + 1)/q + (50) + (51)$ and defining:

$$H = \frac{(2 - \gamma)(S + 1)T}{q} + \psi_O/Y_O + \psi_F/Y_F \quad (52)$$

Zeldovich's H funcion is obtained:

$$St\rho \left[\frac{\partial H}{\partial t} + \vec{v} \cdot \nabla H \right] = \frac{1}{Pe} \nabla \cdot (\rho \alpha H) + \left[\frac{(2-\gamma)(s+1)}{q} \right] \\ \left[(\gamma-1) \frac{1}{Pe} \nabla \cdot (\rho \alpha \nabla T) + \left(\frac{\gamma-1}{Re} \right) \vec{\tau} : \nabla \vec{v} - (\gamma-1) \rho T \nabla \cdot \vec{v} \right] \quad (53)$$

Now, to obtain the Z function of Zeldovich, must sum $-(50) + S \times (51)$, and also defining:

$$Z = SY_F - Y_O + 1 / (S\psi_F - \psi_O + 1)$$

The Z equation is:

$$St\rho \frac{\partial Z}{\partial t} + \rho \vec{v} \cdot \nabla Z = \frac{1}{Pe} \nabla \cdot (\rho \alpha \nabla Z) \quad (54)$$